Kinetic modeling of a one-dimensional, bounded plasma in the ambipolar regime

Monojoy Goswami and H. Ramachandran

Citation: Physics of Plasmas (1994-present) **7**, 4845 (2000); doi: 10.1063/1.1318356
View online: http://dx.doi.org/10.1063/1.1318356
View Table of Contents: http://scitation.aip.org/content/aip/journal/pop/7/12?ver=pdfcov
Published by the AIP Publishing

Kinetic modeling of a one-dimensional, bounded plasma in the ambipolar regime

Monojoy Goswami and H. Ramachandran
Institute for Plasma Research, Bhat, Gandhinagar 382 428, Gujarat, India

(Received 31 May 2000; accepted 21 August 2000)

In this paper we present a self-consistent kinetic simulation of a diffusion dominated bulk plasma region. Collisions have been modeled by a velocity-dependent Krook collision operator. The technique is capable of handling large systems—the results presented here are for systems $100\lambda_{mfp}$ in extent—yet retains the details of the edge physics present. The distribution functions for the trapped and the transiting orbits and their moments are obtained. The density and potential profiles inside the bulk shows overall agreement with ambipolar predictions. The kinetic equivalent of D_A is obtained and compared to the fluid prediction. The validity of the code and the observed deviations from fluid treatments are discussed. © *2000 American Institute of Physics.* [S1070-664X(00)01112-5]

I. INTRODUCTION

The modeling of a glow discharge plasma has its importance in the plasma processing industry, such as in plasma deposition, etching, and processing of semiconductor materials.[1] The transport dominated region of such plasmas are conventionally treated as fluid.[2,3] It is assumed that the distribution functions are nearly Maxwellian and that the behavior is therefore correctly expressible in terms of fluid equations, as given in Ref. 4. The edge region of a plasma is often modeled as fluid, but here the assumption of diffusive flow is questionable due to the presence of a strong field.[5]

There has been a considerable amount of work done in the modeling of the positive column of glow discharge plasma. The first attempt was carried out by Persson,[6] who used fluid theory to solve the ambipolar problem analytically. Using the Boltzmann equation for the electrons and fluid ions Blank[5] treated the positive column for the case of a constant electron–neutral recoil collision time for momentum transfer, in the limit where inelastic collisions play a weak role in determining the shape of the body of the electron distribution function. Bissell and Johnson[7] have solved the plasma equation for a warm collisionless plasma with a Maxwellian particle source in plane parallel geometry. Metze *et al.*[8] have modeled the positive column of a dc discharge for a plasma in a cylindrical system and obtained the radial distribution of ion and electron densities and electric field strength. Their fluid model can be utilized for conditions ranging from the ambipolar diffusion limit to the free diffusion limit. Valentini *et al.*[9] have carried out a generalized fluid study for the positive column for nonemitting electrodes. For a multicomponent plasma Valentini and Herrmann[10] have done a fluid modeling of the boundary value problem. Kouznetsov *et al.*[11] have carried out extensive fluid modeling for the positive column of electronegative plasmas. Recently two-dimensional fluid model of an inductively coupled plasma has been carried out by Bukowski.[12] They have compared their data with experimental spatial profiles, which shows nice agreement between experiment and modeling. Gudmundsson and Lieberman[13] have modeled a planar inductive oxygen discharge using fluid theory and compared their result with experiments. Their fluid modeling shows good agreement with experiments. A pseudospectral discretization method based on polynomial trial functions have been used by Lin *et al.*[14] to solve a self-consistent dc discharge model and have studied the interplay between modeling assumptions and convergence of the numerical solution techniques.

Issues that still remain unclear are the following.

(1) How valid is it to model source-driven ions via fluid equations?
(2) What is the equation of state for ions in the bulk region?
(3) What is the kinetically correct expression for the ambipolar diffusion coefficient?
(4) How accurately can a kinetic code pin down such coefficients, i.e., what are the errors present in the numerically computed values?
(5) What nonfluid effects, if any, are present?

In a previous treatment of this problem, the authors carried out a one-dimensional fluid treatment of a bounded, weakly ionized plasma that included diffusion and flow both in the bulk and in the collisional presheath region.[15] The finding was that ambipolar predictions are indeed good in the center of the plasma but fail near the edge. However, near the edge, fluid theory itself is invalid (see, for example, Ref. 4). A kinetic treatment of the same problem was therefore carried out using a particle conserving Krook collision operator.[16] This paper is the first report on the treatment, and in it we discuss the nature of plasma equilibria in the center of the plasma.

The paper is organized as follows. In Sec. II we describe the model assumed for the plasma system and develop the equations to be solved. In Sec. III we develop a third-order accurate analytic approximation to the kernel of the equation developed in Sec. II. In Sec. IV we discuss the numerical algorithm followed in the code. In Sec. V we present the

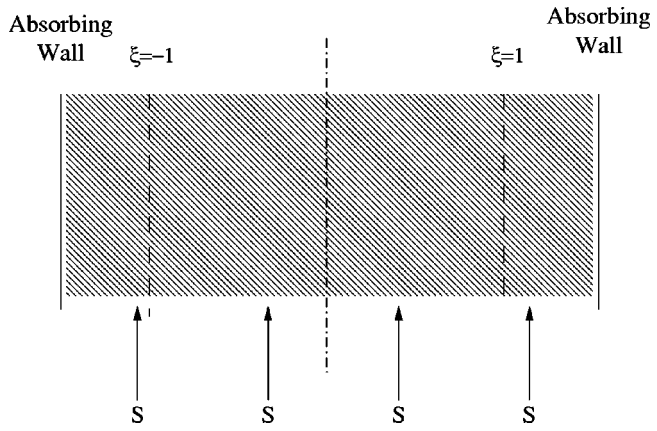

FIG. 1. Model of system assumed in this paper. A one-dimensional plasma is confined between walls, which are assumed electrically floating. The region of analysis is well inside the bulk plasma, A distributed source is present throughout the system.

results and discuss the validity issues and conclude the paper by summarizing the implications for ambipolar treatments of plasmas.

II. MODEL EQUATIONS

The model problem under study consists of a bounded one-dimensional, kinetic plasma, under steady-state (time-independent) conditions, as presented in Fig. 1. The plasma is assumed to be one where ion–neutral collisions dominate, and where the electrons are collisional enough to be thermalized. The equations are only valid in the quasineutral plasma, and the sheath region itself is assumed to be ideal. As indicated in the figure, the code is also capable of simulating a portion of the plasma column. The terminating boundaries are assumed to be floating electrically and zero current is assumed to flow to the walls. A uniform source is assumed present throughout the plasma column, and the source is assumed to inject a stationary Maxwellian distribution of particles at temperature T_0. Shaped and non-Maxwellian sources are within the capability of the code, but are not discussed here.

The ions are modeled as kinetic and subject to a Krook collision operator[16] as well as a source:

$$M\frac{df(\xi,M)}{d\xi}-\frac{d\psi(\xi)}{d\xi}\frac{df(\xi,M)}{dM}=-\nu_i(\xi,M)[f-n(\xi)g_0(M)]+S(\xi,M), \tag{1}$$

where $f(\xi,M)$ is the one-particle distribution function of ions and $\xi=x/L$ and $M=v/c_s$ are the position and velocity coordinates, respectively, normalized to the machine size L and the ion-acoustic velocity $c_s=\sqrt{T_e/m_i}$. Here $\psi=e\phi/T_e$ is the electrostatic potential normalized to the the electron temperature (assumed constant). Here S is the source distribution function and g_0 is a unit density Maxwellian distribution with zero drift and temperature T_0 (representing the temperature of the neutral background and assumed constant). Also, ν_i is the collision cross section for ion–neutral collisions. The collision operator conserves particles if $n(\xi)=\int \nu_i f(M)\mathrm{d}M/\int \nu_i g(M)\mathrm{d}M$. For the results reported in this paper, $n(\xi)$ has been taken to be the number density of ions, $\int f(M)\mathrm{d}M$. The consequence is that the collision operator itself is also a source (or sink) of particles, and the total source is the sum of the explicit source and the collisional source. This is further discussed in Sec. V.

Equation (1) may be solved for f along the characteristics of the orbits, which are just lines of constant energy. It is worth noting here that the characteristics of Eq. (1) are *not* the single-particle orbits of ions in this system. An ion in this system would experience drag and would slow down, thus losing energy. The characteristics of Eq. (1), on the other hand, correspond to the orbit of a drag-free ion. Equation (1) then becomes

$$\frac{df(\tau;\xi_1,E)}{d\tau}+\nu_i(\tau;\xi_1,E)f(\tau;\xi_1,E)=\nu_i(\tau;\xi_1,E)n(\tau;\xi_1,E)g_0(\tau;\xi_1,E)+S(\tau;\xi_1,E), \tag{2}$$

where $\tau=c_s(t-t_1)/L$ is the Lagrangian time normalized to L/c_s and ξ_1 is the initial value of ξ. Equation (2) is an ordinary differential equation that is easily solved to yield

$$f(\xi,E)=\int_{\xi_1}^{\xi}\left(\frac{S(\xi',E)}{\nu(\xi',E)}+n(\xi')g[M(\xi',E)]\right)\times\left[\frac{\nu(\xi',E)}{M(\xi',E)}\exp\left(-\int_{\xi'}^{\xi}\frac{\nu(\xi'',E)}{M(\xi'',E)}\mathrm{d}\xi''\right)\right]\mathrm{d}\xi'+f(\xi_1,E)\exp\left(-\int_{\xi_1}^{\xi}\frac{\nu(\xi'',E)}{M(\xi'',E)}\mathrm{d}\xi''\right), \tag{3}$$

where τ has been transformed back to ξ using $\mathrm{d}\tau=\mathrm{d}\xi/M$. Equation (3) is valid both for $\xi>\xi_1$ and for $\xi_1>\xi$, since $(\xi-\xi_1)/M>0$ always holds, i.e., f is calculated based on information received earlier in Lagrangian time.

The collision frequency is assumed to have a velocity dependence of the following form:

$$\nu(\xi,E)=\nu_0\left(1+\frac{M(\xi,E)}{\bar{M}}\right), \tag{4}$$

where $\bar{M}=\sqrt{T_i/T_e}$ is the normalized ion thermal velocity, and $2\nu_0$ is the ion–neutral collision frequency for thermal ions. This model yields a constant λ_{mfp} for fast ions, consistent with the idea of scattering off a random collection of stationary scattering points, while it yields a constant ν for slow ions, consistent with the idea of collisions experienced by a stationary particle in an ideal gas. For this treatment, ν_0 is assumed independent of position.

III. APPROXIMATING THE KERNEL

Equation (3) is numerically expensive to compute as it is a double integral. This double integral can be reduced to two single integrals by recognizing the expression as a convolution. However, the resulting expression involves the ratio of two exponential terms with large exponents, causing numerical inaccuracies and overflow (or underflow) problems. The approach used in this paper has been to obtain an analytic approximation for the kernel of the integral in Eq. (3),

$$\Lambda(\xi,\xi',E)=\frac{\nu(\xi',E)}{M(\xi',E)}\exp\left(-\int_{\xi'}^{\xi}\frac{\nu(\xi'',E)}{M(\xi'',E)}d\xi''\right), \quad (5)$$

thereby short-circuiting much of the computational overhead. The expression obtained below is correct to $\mathcal{O}[(\xi-\xi')^3]$, and the resulting errors must be tracked and kept within the required limits.

The potential profile is first approximated to second order, about a point $\xi=\xi_0$:

$$\psi(\xi)=\frac{\psi_0''}{2}\left[\left((\xi-\xi_0)+\frac{\psi_0'}{\psi_0''}\right)^2+\frac{2\psi_0}{\psi_0''}-\left(\frac{\psi_0'}{\psi_0''}\right)^2\right]+\mathcal{O}[(\xi-\xi_0)^3]. \quad (6)$$

The orbit velocity, $M(\xi,E)=v/c_s=\sqrt{2(E-\psi)}$ may therefore be approximated to second order as

$$\frac{M^2(\xi,E)}{2}=\left(E-\psi_0+\frac{\psi_0'^2}{2\psi_0''}\right)+\left(\frac{-\psi_0''}{2}\right)\left(\xi-\xi_0+\frac{\psi_0'}{\psi_0''}\right)^2+\mathcal{O}[(\xi-\xi_0)^3]. \quad (7)$$

These expressions for M and ψ are valid even near the peak where the potential becomes flat, due to the condition $\psi''<0$ in an ambipolar plasma.

Assuming that ν_0 is not a function of position, the exponent in Eq. (3) can be approximated using Eq. (7),

$$\int_{\xi'}^{\xi}\frac{\nu}{M}d\xi''=\frac{\nu_0}{\sqrt{2}}\int_{\xi'}^{\xi}\frac{1}{\sqrt{(E-\psi_0+\psi_0'^2/2\psi_0'')+(-\psi_0''/2)(\xi''-\xi_0+\psi_0'/\psi_0'')^2}}d\xi''+\frac{\nu_0}{\bar{M}}(\xi-\xi')+\mathcal{O}[(\xi-\xi_0)^3]. \quad (8)$$

Transforming to $u=\xi''-\xi_0+\psi_0'/\psi_0''$ yields

$$\int_{\xi'}^{\xi}\frac{\nu}{M}d\xi''=\frac{\nu_0}{\bar{M}}(\xi-\xi')+\nu_0\sqrt{\frac{1}{-\psi_0''}}\ln\left|\frac{\zeta(\xi-\xi_0+\psi_0'/\psi_0'')}{\zeta(\xi'-\xi_0+\psi_0'/\psi_0'')}\right|+\mathcal{O}[(\xi-\xi_0)^3], \quad (9)$$

where $\zeta(x)$ is defined by

$$\zeta(x)=x+\sqrt{x^2+\left(E-\psi_0+\frac{\psi_0'^2}{2\psi_0''}\right)\frac{2}{-\psi_0''}}. \quad (10)$$

Comparing Eq. (8) and Eq. (10), it is clear that

$$\zeta(\xi''-\xi_0+\psi_0'/\psi_0'')=\xi''-\xi_0+\psi_0'/\psi_0''+\sqrt{\frac{2}{-\psi_0''}}M(\psi''). \quad (11)$$

As long as $E>\psi(\xi'')$ is nonzero in $\xi'<\xi''<\xi$, ζ is also well defined in Eq. (9). The difference between ''trapped'' and ''transiting'' orbits lies in whether the potential peak rises above the value of E or not. In this local approximation treatment, that is equivalent to whether $E-\psi_0+\psi_0'^2/2\psi_0''$ is positive or negative. In either case, Eq. (9) is valid and, hence, the treatment is independent of the type of orbit. Thus, Eq. (3) may be written as

$$f(\xi,E)=\int_{\xi_<}^{\xi_>}\Lambda(\xi',\xi,E)\left(\frac{S}{\nu}+ng\right)d\xi'+f(\xi_1,E)\Lambda(\xi_1,\xi,E)\frac{|M(\xi_1,E)|\bar{M}}{\nu_0(|M(\xi_1,E)|+\bar{M})}, \quad (12)$$

where $\xi_<$ and $\xi_>$ denote, respectively, the algebraically smaller and greater of ξ, ξ_1 and Λ is given by

$$\Lambda(\xi,\xi',E)=e^{-\nu_0(|\xi-\xi'|/\bar{M})}\nu_0\left(\frac{1}{|M(\xi',E)|}+\frac{1}{\bar{M}}\right)\times\left(\frac{\zeta(\xi-\xi_0+\psi_0'/\psi_0'')}{\zeta(\xi'-\xi_0+\psi_0'/\psi_0'')}\right)^{\pm\nu_0/\sqrt{-\psi_0''}}+\mathcal{O}[(\xi-\xi_0)^3], \quad (13)$$

where the sign of the exponent is chosen to keep the ζ ratio less than unity. It should be noted that Λ is not symmetric in its first two arguments, due to the explicit presence of $|M(a,E)|$ in Eq. (13). Here $\Lambda(\xi,\xi')$ has the property that it is integrable, even when $M\to 0$. Consider the situation where $\psi'\neq 0$. The potential is expanded about the turning point ξ_0, which is one of ξ or ξ'. The ratio of ζ terms in Eq. (13) then reduces to (with $\tilde{\xi}$ denoting the nonsingular end point)

$$\left(\frac{\psi_0'/\psi_0''}{\zeta(\tilde{\xi}-\xi_0+\psi_0'/\psi_0'')}\right)^{\pm\nu_0/\sqrt{-\psi_0''}}, \quad (14)$$

which is a regular expression. For this case, the only singularity comes from $1/M(\xi',E)$, which is in agreement with Eq. (5). When $\psi'\neq 0$, $M\propto\sqrt{\xi-\xi_0}$, which means that Λ has a square root singularity at $\xi\to\xi_0$, which is integrable by the transformation $\pm u^2=\xi-\xi_0$.

If $\psi'=0$ at the turning point, then it is clear from Eq. (11) that $\zeta(\xi)\propto(\xi-\xi_0)$ and similarly from Eq. (16) that $M(\xi)\propto(\xi-\xi_0)$. Hence, Eq. (13) reduces to

$$\Lambda\propto\frac{1}{\xi'-\xi_0}\left(\frac{\xi-\xi_0}{\xi'-\xi_0}\right)^{\pm\nu_0/\sqrt{-\psi_0''}}. \quad (15)$$

Depending upon the location of the singularity, either $\Lambda \propto (\xi' - \xi_0)^{(\nu_0/\sqrt{-\psi_0''})-1}$, or $\Lambda \propto (\xi - \xi_0)^{\nu_0/\sqrt{-\psi_0''}}$. Clearly this expression is integrable as long as the power of $\xi - \xi_0$ is greater than -1.0. The interpretation of this result is that collisions are required to prevent the distribution function from being overwhelmed by the effective source of particles, $S + \nu n g$, at low velocities. This is because particles spend a long time in these low-velocity characteristics and therefore experience a strong fueling from the sources. Only collisions can expel these particles from this portion of phase space and keep the distribution function from becoming singular.

IV. IMPLEMENTATION SCHEME FOR KINETIC CODE

Equation (13) is a second-order accurate expression for $\Lambda(\xi, \xi', E)$, where ψ_0, ψ_0', and ψ_0'' are the value, first, and second derivative, respectively, of ψ at some $\xi = \xi_0$. It is valid as long as the location of $M(\xi, E) = 0$ lies outside (or, at most, on the boundary) of the region of integration. For Eq. (9) to be accurate, if M goes to zero in the vicinity of the region being integrated over, that point should be taken as ξ_0, the Taylor expansion point. To use Eq. (13) in Eq. (12), it is necessary to approximate $M(\xi, E)$ by

$$M(\xi, E) = \sqrt{E - \psi_0 + \frac{\psi_0'^2}{2\psi_0''} - \frac{\psi_0''}{2}\left(\xi - \xi_0 + \frac{\psi_0'}{\psi_0''}\right)^2}, \quad (16)$$

wherever it occurs explicitly in Eq. (12) as well.

From a computational point of view, the issue is to determine the scheme of integration depending on the nature of the orbit and the proximity to a singular point. There are three general cases to consider.

(1) A region where the velocity does not got to zero. Then the integral may be done directly.
(2) A region including the location where ψ reaches its maximum value. Here, even though the velocity goes to zero, Λ remains bounded, and well behaved, as long as $\lambda_{\text{mfp}}^2 < 1/-\psi_0''$, i.e., the collision scale length is smaller than the transport scale length in the bulk. So, the integral may be done directly here as well.
(3) A region where one of the end points is a turning point, i.e., where $E = \psi$ and ψ' is nonzero. Then, the integral must be done taking the square root singularity into account.

In cases 1 and 2, a Romberg integration scheme is used to calculate f from Eq. (12). In case 3, Romberg integration is carried out after transforming the integrand according to the transformation given below Eq. (14).

Since the problem treated in this paper is the simulation of an internal portion of a plasma, the boundaries of the simulation are made emissive. Specifically, the boundaries are made to emit drifting Maxwellian distributions whose amplitude, drift and temperature are matched to the edge plasma itself:

$$f_W(M) = n_W \sqrt{\frac{1}{2\pi\tau}} \exp\left(-\frac{(M - M_d)^2 \tau}{2}\right), \quad (17)$$

TABLE I. Parameters assumed in the runs.

Parameter	Value	Type
Mass ratio	1836	Fixed
D_A	0.0156	Fixed
n_0	81.9	Fixed
T_e/T_i	0.5–10.0	Varied
λ_{mfp}	—	Solved for

where $\tau = T_e/T_0$ is the temperature ratio. n_W and M_d have the additional constraint that they conserve particles over all, i.e., $n_W M_d = \int_0^1 S_{\text{eff}} d\xi$. S_{eff} here is the effective source, as discussed below Eq. (1).

Equation (12) is solved in $-1 < \xi < 1$ and $\psi_{\min} < E < E_{\max}$ at a set of ξ locations selected suitably to keep the error from the use of Eq. (13) within bounds. The set of E values at which solutions are obtained is selected to control the error in the calculation of moments of f. The choice of $E_{\max}$ is made by determining the error in the moments due to the neglect of contributions from $E > E_{\max}$ in Eq. (3),

$$\int_{M_{\max}}^{\infty} M^k f(\xi, M) dM \leqslant \left(\frac{S_{\max}}{\nu_0} + n_{\max}\right) \int_{M_{\max}}^{\infty} M^k g(M) dM + \int_{M_{\max}}^{\infty} M^k f_{\text{Edge}}(M) dM. \quad (18)$$

For the problem considered, convergence requires the zeroth and first moments, i.e., $k = 0,1$.

The electrostatic potential is obtained from the moments of the distribution via the electron equation. The electrons are treated as a collisional, inertia-less fluid, which yields [Eq. (22) in Ref. 15)]

$$\psi(\xi) = \psi(0) + \ln\left(\frac{n(\xi)}{n(0)}\right) + \nu_0 \sqrt{\frac{m_e T_e}{m_i T_i}} \int_0^{\xi} M(\xi') d\xi'. \quad (19)$$

This completes the system of equations that are iteratively solved for until convergence is obtained.

V. RESULTS AND DISCUSSIONS

The procedure described in the previous section was followed and solutions obtained. Since our purpose in the study was to explore the transport-dominated regime of plasma behavior, a parabolic profile for the density was used as a guess. The parabolic solution comes from the ambipolar diffusion equation.[2] The parameters that were used are described in Table I. A density profile with a fixed peak value, n_0, and a fixed curvature, n_0'', was used as the seed to converge the code for various temperature ratios.

Figure 2 displays the profiles for the case of $T_e = 2T_0$. Figure 2(a) shows the density profile, which is a near parabola as required by ambipolar considerations. The velocity profile is displayed in Fig. 2(b). The flow velocities are much smaller than c_s, as required in the transport regime. The temperature profile (not displayed) was found to be constant to four significant digits, confirming the isothermal nature of

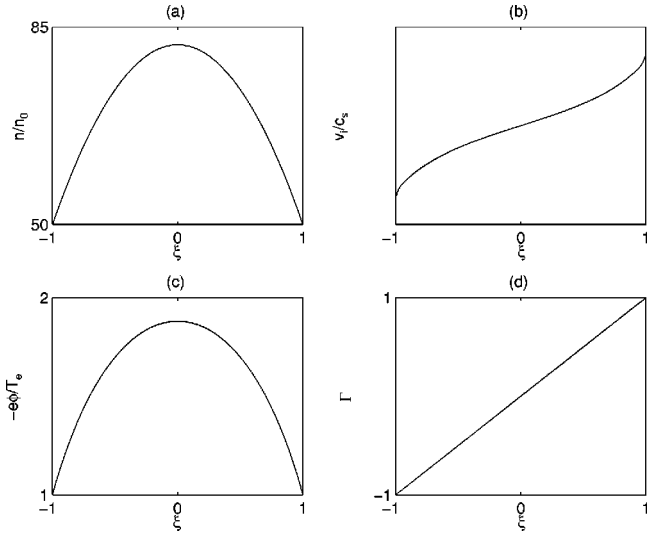

FIG. 2. Self-consistent plasma profiles obtained for the case $T_e = T_i$ and hydrogen plasma. (a) Density profile of the plasma. As expected for an ambipolar system, it is essentially a parabola. (b) Fluid velocity profile, normalized to c_s. (c) Potential profile, normalized to T_e/e. (d) The flux of particles, calculated from plasma quantities. This is a check on the numerical accuracy of the code, as it should be linear.

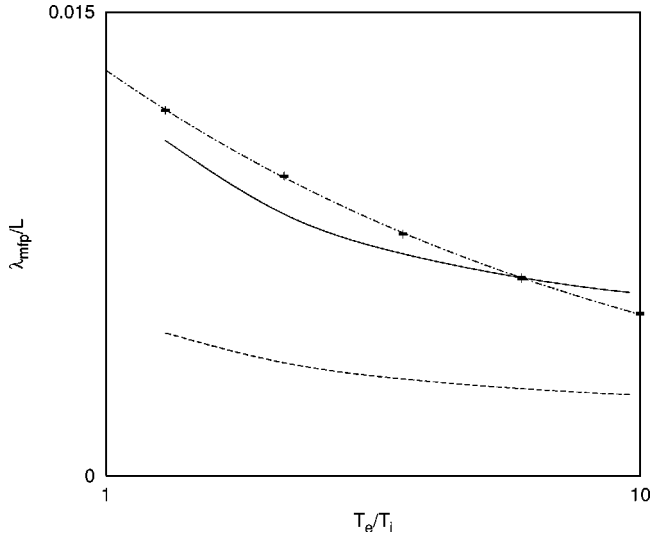

FIG. 3. The λ_{mfp} values obtained from the code for varied temperature ratios. Since the density profile was the same in all cases, the ambipolar diffusion coefficient D_A is also the same. The plus symbols are the λ_{mfp} values required in each case to obtain convergence. The solid line is a plot of Eq. (32). The dashed line is the fluid theory expression for $D_A = \lambda_{\mathrm{mfp}}\sqrt{1+T_e/T_i}/(1+\sqrt{m_e T_e/m_i T_i})$, with λ_{mfp} adjusted to give a best fit. The dot–dashed line is the function $0.0145\exp(-T_e/9.768T_i)$ fitted to the numerical data.

the plasma. The potential profile is displayed in Fig. 2(c). Figure 2(d) displays the particle flux as a function of position. The quantity plotted is actually

$$\int_{-\infty}^{\infty}\left(Mf(\xi,M)+\int_0^{\xi}\nu(M)[f(\xi',M) - n(\xi')g(M)]\mathrm{d}\xi'\right)\mathrm{d}M. \tag{20}$$

From Eq. (1), for a uniform, Maxwellian source of unit amplitude, this quantity should be exactly ξ.

The density profile was converged for different temperature ratios. Convergence was obtained with the *same* density profile though with different λ_{mfp} when the temperature ratio was changed from 0.5 to 16. Table II displays the relative errors in the calculation of density, velocity and particle flux for these runs. The errors were defined as the root-mean-square relative errors in the quantities. The deviation of the calculated particle flux from its theoretical value of $\Gamma = \xi$ provides a means to check the accuracy of the code. The observed accuracies were found to be consistent with the accuracy of the individual algorithms in the code.

TABLE II. Relative error in density, velocity and flux for different temperature ratios.

T_e/T_i	$\Delta n/n$	$\Delta v/v$	$\Delta\Gamma/\Gamma$
1.0	8.0×10^{-5}	1.5×10^{-3}	0.0025
2.0	3.0×10^{-4}	9.0×10^{-3}	0.0025
4.0	3.5×10^{-4}	7.0×10^{-3}	0.0040
5.0	4.5×10^{-4}	7.0×10^{-3}	0.005
6.0	5.5×10^{-4}	6.0×10^{-3}	0.0080
8.0	7.0×10^{-4}	6.5×10^{-3}	0.021
10.0	6.0×10^{-4}	5.0×10^{-3}	0.055

Since the density profile was a parabola in these runs, the second derivative of the density was fixed. Thus, the ambipolar diffusion coefficient was known. For this situation, Fig. 3 displays the variation of λ_{mfp} with the temperature ratio, $\tau = T_e/T_i$. The plus symbols are the actual values obtained by converging the kinetic code. The corresponding fluid expression linking λ_{mfp} and D_A is [Eq. (B3) in Ref. 15]:

$$D_A = \frac{\bar{M}^2}{\nu_0}\frac{1+T_e/T_i}{1+\sqrt{m_e T_e/m_i T_i}}. \tag{21}$$

The dashed line in Fig. 3 is obtained from this formula. This fluid relationship has a kinetic equivalent. At the peak of the density profile (i.e., at $\xi = 0$), the distribution function can be approximately solved using Eq. (3),

$$f(\xi,v)\approx\int_{\tau_W}^{\tau}\left[\left(n+\frac{S_0}{\nu}\right)g\Big|_0 + \left[\left(n+\frac{S_0}{\nu}\right)g\right]''\Big|_0\frac{(\xi-\xi')^2}{2}\right]e^{-(\tau-\tau')}\mathrm{d}\tau', \tag{22}$$

where the profiles have been expanded to second order in ξ about $\xi = 0$, the contribution from the initial condition ignored (since $L \gg \lambda_{\mathrm{mfp}}$), and the integral transformed to $(\tau - \tau_W) = \int_{\xi_W}^{\xi}\nu/M\,\mathrm{d}\xi'$, which is the Lagrangian time normalized to inverse collision frequency. Equation (22) can be rewritten as

$$f(\xi,v)\approx\left(n+\frac{S_0}{\nu}\right)g\Big|_0 + \left[\left(n+\frac{S_0}{\nu}\right)g\right]''\Big|_0 \times\int_{\tau_W}^{\tau}\frac{(\xi-\xi')^2}{2}e^{-(\tau-\tau')}\mathrm{d}\tau'. \tag{23}$$

The value of v along the orbit can be connected to the value of ξ using Eq. (7), and the second derivative can be evaluated at $\xi=0$:

$$\left[\left(n+\frac{S_0}{\nu}\right)g\right]''\Big|_0 \simeq n''g+\left(n+\frac{S_0}{\nu}\right)\left(-\frac{M^2}{\bar{M}^2}\right)\frac{-\psi''/2}{E-\psi_0}g, \tag{24}$$

where the variation of ν along the orbit has been neglected, as it is multiplied by $S_0 \ll \nu_0 n$. The connection between $\xi-\xi'$ and $\tau-\tau'$ comes from the differential relation

$$d\tau=\frac{\nu}{M}d\xi. \tag{25}$$

Assuming that M does not change significantly over a λ_{mfp}, this yields

$$\xi-\xi'=\frac{|M|\bar{M}}{\nu_0(|M|+\bar{M})}(\tau-\tau')+\mathcal{O}\left(\frac{\bar{M}^3\psi''}{\nu_0^3}(\tau-\tau')^3\right), \tag{26}$$

i.e.,

$$\int_{\tau_0}^{\tau}\frac{(\xi-\xi')^2}{2}e^{-(\tau-\tau')}\mathrm{d}\tau' \approx \frac{\lambda_{\mathrm{mfp}}^2}{2}\int_{\tau_0}^{\tau}(\tau-\tau')^2e^{-(\tau-\tau')}\mathrm{d}\tau' = \lambda_{\mathrm{mfp}}^2, \tag{27}$$

where $1/\lambda_{\mathrm{mfp}}=\nu_0(1/|M|+1/\bar{M})$. Equation (23) can now be written as

$$f(\xi,M)\approx\left(n+\frac{S_0}{\nu}\right)g+\lambda_{\mathrm{mfp}}^2 g\left[n''+\left(n+\frac{S_0}{\nu}\right)\frac{M^2}{\bar{M}^2}\frac{\psi''/2}{E-\psi}\right]. \tag{28}$$

The S_0/ν term is small compared to n in a highly collisional system and may be ignored in the coefficient of ψ''. It must be retained elsewhere due to cancellation effects. Boltzmann electrons connect $e\phi$ and n via $n''=en\phi''/T_e$. Then Eq. (28) becomes

$$f(\xi,M)\approx\left(n+\frac{S_0}{\nu}\right)g+\lambda_{\mathrm{mfp}}^2 g n''\left(1+\frac{T_e}{T_i}\right). \tag{29}$$

The profile for n in Eq. (29) is actually the guessed profile, $\tilde{n}$, which is different from $n=\int f\mathrm{d}M$. Using Eq. (29), the effective source due to the collision operator is obtained:

$$\int -\nu(f-\tilde{n}g)\mathrm{d}M=-\tilde{n}\int \nu g\mathrm{d}M-S_0-\int \nu\lambda_{\mathrm{mfp}}^2\left(1+\frac{T_e}{T_i}\right)\times g(M)\tilde{n}''\mathrm{d}M+\tilde{n}\int \nu g\mathrm{d}M, \tag{30}$$

i.e.,

$$\frac{\left(1+\frac{T_e}{T_i}\right)\langle\nu\lambda_{\mathrm{mfp}}^2\rangle}{1-\frac{1}{S_0}\int\nu(f-\tilde{n}g)\mathrm{d}M}\tilde{n}''=-S_0. \tag{31}$$

This has the form of a diffusion equation. Here $\langle\nu\lambda_{\mathrm{mfp}}^2\rangle=\langle|M|\lambda_{\mathrm{mfp}}\rangle$ can be evaluated, to yield

$$\frac{\left(1+\frac{T_e}{T_i}\right)\sqrt{\frac{2}{\pi}}\bar{M}\lambda_{\mathrm{mfp}}\left(1-\sqrt{\frac{\pi}{2}}+\int_0^{\infty}\frac{\exp(-t^2/2)}{t+1}\mathrm{d}t\right)}{1-\frac{1}{S_0}\int\nu(f-\tilde{n}g)\mathrm{d}M}\tilde{n}'' = -S_0. \tag{32}$$

The integral has the value 0.770 625 939 8 to ten digits. The value of $\int\nu(f-\tilde{n}g)\mathrm{d}M$ is numerically obtained by the code, which yields a value of D_A.

It should be noted that away from $\xi=0$, the neglected first derivative terms are nonzero and there are (nonlinear) corrections to Eq. (32). Equation (32) was used to predict λ_{mfp} for varied T_e/T_i. The solid line in Fig. 3 is the resulting prediction. As is clear from the figure, the agreement with numerics is superior to the fluid result. The improved fit lies primarily in the accurate calculation of the value of $\langle\lambda_{\mathrm{mfp}}|M|\rangle$, where the actual velocity dependence of ν was taken into account. However, there are still clear deviations from the numerical data. These deviations are not understood at present.

In conclusion, a fully self-consistent, one-dimensional, kinetic code has been developed that can analyze ''large systems'' (i.e., systems that are many mean-free paths in extent). The code is able to reproduce bulk plasma behavior predicted from fluid and kinetic theory, with some deviations. These deviations are clearly larger than the errors in the code and require further study. Perhaps most intriguing is the empirical fit of the numerical λ_{mfp} data to a decaying exponential in T_e/T_i. Future work will report on the findings of this code for a system in contact with boundaries.

[1] M. A. Lieberman and A. J. Lichtenberg, *Principles of Plasma Discharges and Materials Processing* (Wiley, New York, 1994).
[2] F. F. Chen, *Plasma Physics*, Plasma Physics and Controlled Fusion (Plenum, New York, 1984), Vol. 1, Chap. 5, p. 55.
[3] R. N. Franklin, *Plasma Phenomena in Gas Discharges* (Clarendon, Oxford, 1976), Chap. 4, p. 51.
[4] K.-U. Riemann, J. Phys. D **24**, 493 (1991).
[5] J. B. Blank, Phys. Fluids **11**, 1686 (1968).
[6] K. B. Persson, Phys. Fluids **5**, 1625 (1962).
[7] R. C. Bissell and P. C. Johnson, Phys. Fluids **30**, 779 (1987).
[8] A. Metze, D. W. Ernie, and H. J. Oskam, Phys. Rev. A **39**, 4117 (1989).
[9] H-B. Valentini, E. Glauche, and D. Wolff, Plasma Sources Sci. Technol. **4**, 353 (1995).
[10] H-B. Valentini and F. Herrmann, J. Phys. D **29**, 1175 (1996).
[11] I. G. Kouznetsov, A. J. Lichtenberg, and M. A. Lieberman, Plasma Sources Sci. Technol. **5**, 662 (1996).
[12] J. D. Bukowski, D. B. Graves, and P. Vitello, J. Appl. Phys. **80**, 2614 (1996).
[13] J. T. Gudmundsson and M. A. Lieberman, Plasma Sources Sci. Technol. **7**, 1 (1998).
[14] Y. Lin and A. R. Adomaitis, Phys. Lett. A **243**, 142 (1998).
[15] M. Goswami and H. Ramachandran, Phys. Plasmas **6**, 4522 (1999).
[16] P. L. Bhatnagar, E. P. Gross, and M. Krook, Phys. Rev. **94**, 511 (1954).